A wavelet-based tool for studying non-periodicity

R. Benítez[1], V. J. Bolós[2], M. E. Ramírez[3]

[1] Departamento de Matemáticas,
Centro Universitario de Plasencia, Universidad Extremadura.
Avda. Virgen del Puerto 2, 10600 Plasencia, Spain.
e-mail: rbenitez@unex.es

[2] Departamento de Matemáticas para la Economía y la Empresa,
Facultad de Economía, Universidad de Valencia.
Avda. Tarongers s/n, 46071 Valencia, Spain.
e-mail: vicente.bolos@uv.es

[3] GMV A& D, Spain.
e-mail: mramirez@gmv.com

June 2010

Abstract

This paper presents a new numerical approach to the study of non-periodicity in signals, which can complement the maximal Lyapunov exponent method for determining chaos transitions of a given dynamical system. The proposed technique is based on the continuous wavelet transform and the wavelet multiresolution analysis. A new parameter, the *scale index*, is introduced and interpreted as a measure of the degree of the signal's non-periodicity. This methodology is successfully applied to three classical dynamical systems: the Bonhoeffer-van der Pol oscillator, the logistic map, and the Henon map.

Keywords: Non-periodicity; Wavelets; Chaotic dynamical systems

1 Introduction

In the study of chaotic dynamical systems it is quite common to have bifurcation diagrams that represent, for each value of one or more parameters, the number of periodic orbits of the system. The determination of the parameter values for which the system becomes chaotic is a classical problem within the theory of dynamical systems [1].

Although there is no universally accepted definition of chaos, usually, a bounded signal is considered chaotic if (see [2])

(a) it shows sensitive dependence on the initial conditions, and

(b1) it is non-periodic, or

(b2) it does not *converge* to a periodic orbit.

Usually, chaos transitions in bifurcation diagrams are numerically detected by means of the Maximal Lyapunov Exponent (MLE). Roughly speaking, Lyapunov exponents characterize the rate of separation of initially nearby orbits and a system is thus considered chaotic if the MLE is positive. Therefore, the MLE technique is one that focuses on the sensitivity to initial conditions, in other words, on criterion (a).

As to criteria (b1) and (b2), Fourier analysis can be used in order to study non-periodicity. However chaotic signals may be highly non-stationary, which makes wavelets more suitable [3]. Moreover, compactly supported wavelets are a useful tool in the analysis of non-periodicity in compactly supported signals, as we will see in Corollary 2.

Wavelet theory is a quite recent area of mathematical research that has been applied to a wide range of physical and engineering problems (see, for instance [4, 5] for classical applications to image processing and to time series analysis and [6, 7, 8] for examples of non-standard applications to DNA sequences, astronomy and climatology). In particular, the wavelet decomposition of a signal has been proved to be a very useful tool in the study of chaotic systems. Indeed, wavelets have been successfully used in the analysis of the chaotic regimes of the Duffing oscillator, focusing on the detection of periodicities within chaotic signals, and on chaos numerical control (see [9, 10]).

In this paper we present a method for studying non-periodicity that can complement the MLE for determining chaos transitions of a given dynamical system which can be either discrete or continuous. This method is based on the Continuous Wavelet Transform (CWT) and the wavelet Multiresolution Analysis (MRA) of a signal. In particular, we compute the ratio of the scalogram value at the dominant scale (i.e. the scale where the maximum is reached) to the value at the least significant scale (i.e. the scale where the scalogram takes its minimum value after that maximum is reached). This quotient determines the *scale index* which is strictly positive when the signal is non-periodic, and can be interpreted as a measure of the degree of non-periodicity.

The paper is organized as follows: Section 2 is devoted to the establishing of the background and the main results of the wavelet theory used later in the paper. In Section 3 we give an overview of the scalogram and define the scale index. Finally, Section 4 illustrates the value of the method by showing the successfull detection of the chaos transitions for three classical systems: the Bonhoeffer-van der Pol (BvP) oscillator, the logistic map and the Henon map.

2 Wavelet analysis of time series

In this section we introduce the wavelet tools and results needed for defining the *scale index*.

2.1 Continuous wavelet transform and scalogram

Wavelet theory is based on the existence of two special functions ϕ and ψ, known as the *scaling* and *wavelet functions* respectively [11].

A *wavelet function* (or wavelet, for short) is a function $\psi \in L^2(\mathbb{R})$ with zero average (i.e. $\int_{\mathbb{R}} \psi = 0$), with $\|\psi\| = 1$, and *centered* in the neighborhood of $t = 0$ [11]. Moreover, we are going to demand that $t\psi(t) \in L^1(\mathbb{R})$ in order to ensure that the continuous wavelet transform (3) is invertible in some way.

Given a wavelet ψ, its dilated and translated dyadic version is given by

$$\psi_{j,k}(t) := \frac{1}{\sqrt{2^j}} \psi\left(\frac{t - 2^j k}{2^j}\right), \tag{1}$$

where $j, k \in \mathbb{Z}$. It is important to construct wavelets such that the family of dyadic wavelets $\{\psi_{j,k}\}_{j,k\in\mathbb{Z}}$ is an orthonormal basis of $L^2(\mathbb{R})$. These orthonormal bases are related to the Multiresolution Analysis (MRA) of signals.

Scaling ψ by a positive quantity s, and translating it by $u \in \mathbb{R}$, we define a family of *time–frequency atoms*, $\psi_{u,s}$, as follows:

$$\psi_{u,s}(t) := \frac{1}{\sqrt{s}} \psi\left(\frac{t - u}{s}\right), \qquad u \in \mathbb{R},\ s > 0. \tag{2}$$

Note that there is an abuse of notation in expressions (2) and (1).

Given $f \in L^2(\mathbb{R})$, the *continuous wavelet transform* (CWT) of f at time u and scale s is defined as

$$Wf(u, s) := \langle f, \psi_{u,s} \rangle = \int_{-\infty}^{+\infty} f(t) \psi^*_{u,s}(t) \mathrm{d}t, \tag{3}$$

and it provides the frequency component (or *details*) of f corresponding to the scale s and time location t.

The wavelet transform given in (3), provides a time–frequency decomposition of f in the so called *time–frequency plane* (see Figure 1).

The *scalogram* of f, $\mathcal{S}$, is defined as follows:

$$\mathcal{S}(s) := \|Wf(u, s)\| = \left(\int_{-\infty}^{+\infty} |Wf(u, s)|^2 \mathrm{d}u \right)^{\frac{1}{2}}.$$

$\mathcal{S}(s)$ is the *energy* of the continuous wavelet transform of f at scale s. Obviously, $\mathcal{S}(s) \geq 0$ for all scale s, and if $\mathcal{S}(s) > 0$ we will say that the signal f has details at scale s. Thus, the scalogram is a useful tool for studying a signal, since it allows the detection of its most representative scales (or frequencies), that is, the scales that mostly contribute to the total energy of the signal.

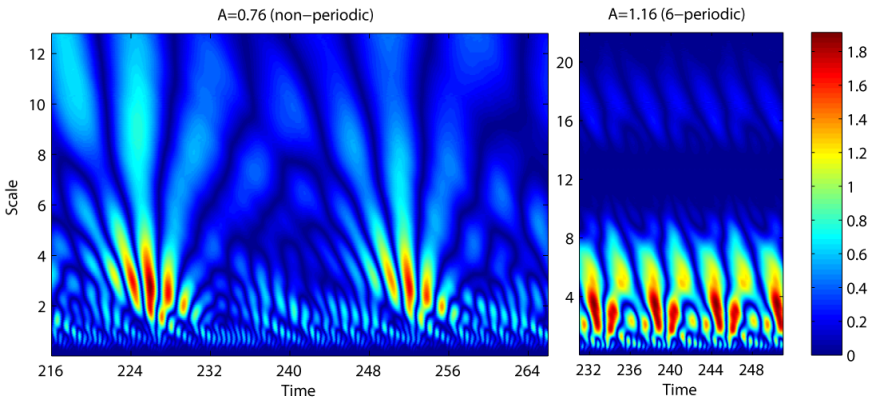

Figure 1: Time–frequency plane decomposition corresponding to the BvP solution with $A = 0.76$ (left) and $A = 1.16$ (right) using Daubechies (eight–wavelet and four–wavelet respectively) wavelet functions (see Section 4.1 for the definition of the BvP system). Each point in this 2D representation corresponds to the modulus of the wavelet coefficients of the CWT. Note that the wavelet coefficients of the CWT with $A = 1.16$ vanish at scale 12 (i.e. twice its period) at any time, as we will prove in Theorem 1.

2.2 Analysis of compactly supported discrete signals

In practice, to make a signal f suitable for a numerical study, we have to

(i) consider that it is defined over a finite time interval $I = [a, b]$, and

(ii) sample it to get a discrete set of data.

Regarding the first point, boundary problems arise if the support of $\psi_{u,s}$ overlaps $t = a$ or $t = b$. There are several methods for avoiding these problems, like using *periodic wavelets*, *folded wavelets* or *boundary wavelets* (see [11]); however, these methods either produce large amplitude coefficients at the boundary or complicate the calculations. So, if the wavelet function ψ is compactly supported and the interval I is big enough, the simplest solution is to study only those wavelet coefficients that are not affected by boundary effects.

Taking into account the considerations mentioned above, the *inner scalogram* of f at a scale s is defined by

$$\mathcal{S}^{\text{inner}}(s) := \|Wf(s,u)\|_{J(s)} = \left(\int_{c(s)}^{d(s)} |Wf(s,u)|^2 \mathrm{d}u\right)^{\frac{1}{2}},$$

where $J(s) = [c(s), d(s)] \subseteq I$ is the maximal subinterval in I for which the support of $\psi_{u,s}$ is included in I for all $u \in J(s)$. Obviously, the length of I must be big enough for $J(s)$ not to be empty or too small, i.e. $b - a \gg sl$, where l is the length of the support of ψ.

Since the length of $J(s)$ depends on the scale s, the values of the inner scalogram at different scales cannot be compared. To avoid this problem, we can *normalize* the inner scalogram:

$$\overline{\mathcal{S}}^{\text{inner}}(s) = \frac{\mathcal{S}^{\text{inner}}(s)}{(d(s) - c(s))^{\frac{1}{2}}}.$$

With respect to the sampling of the signal, any discrete signal can be analyzed in a *continuous way* using a piecewise constant interpolation. In this way, the CWT provides a scalogram with a better resolution than the Discrete Wavelet Transform (DWT), that considers dyadic levels instead of continuous scales (see [11]).

3 The scale index

In this section we introduce a new parameter, the *scale index*, that will give us information about the degree of non-periodicity of a signal. To this end we will first state some results for the wavelet analysis of periodic functions (for further reading please refer to [11] and references therein).

If $f : \mathbb{R} \to \mathbb{C}$ is a T-periodic function in $L^2([0,T])$, and ψ is a compactly supported wavelet, then $Wf(u,s)$ is well-defined for $u \in \mathbb{R}$ and $s \in \mathbb{R}^+$, although f is not in $L^2(\mathbb{R})$.

The next theorem gives us a criterion for distinguishing between periodic and non-periodic signals. It ensures that if a signal f has details at every scale (i.e. the scalogram of f does not vanish at any scale), then it is non-periodic.

Theorem 1 *Let $f : \mathbb{R} \to \mathbb{C}$ be a T-periodic function in $L^2([0,T])$, and let ψ be a compactly supported wavelet. Then $Wf(u,2T) = 0$ for all $u \in \mathbb{R}$.*

For a detailed proof see Appendix A. From this result we obtain the following corollary.

Corollary 2 *Let $f : I = [a,b] \to \mathbb{C}$ a T-periodic function in $L^2([a,a+T])$. If ψ is a compactly supported wavelet, then the (normalized) inner scalogram of f at scale $2T$ is zero.*

These results constitute a valuable tool for detecting periodic and non-periodic signals, because a signal with details at every scale must be non-periodic (see Figure 2). Note that in order to detect numerically wether a signal *tends to be periodic*, we have to analyze its scalogram throughout a relatively wide time range.

Moreover, since the scalogram of a T-periodic signal vanishes at all $2kT$ scales (for all $k \in \mathbb{N}$), it is sufficient to analyze only scales greater than a fundamental scale s_0. Thus, a signal which has details at an arbitrarily large scale is non-periodic.

In practice, we shall only study the scalogram on a finite interval $[s_0, s_1]$. The most representative scale of a signal f will be the scale $s_{\max}$ for which the

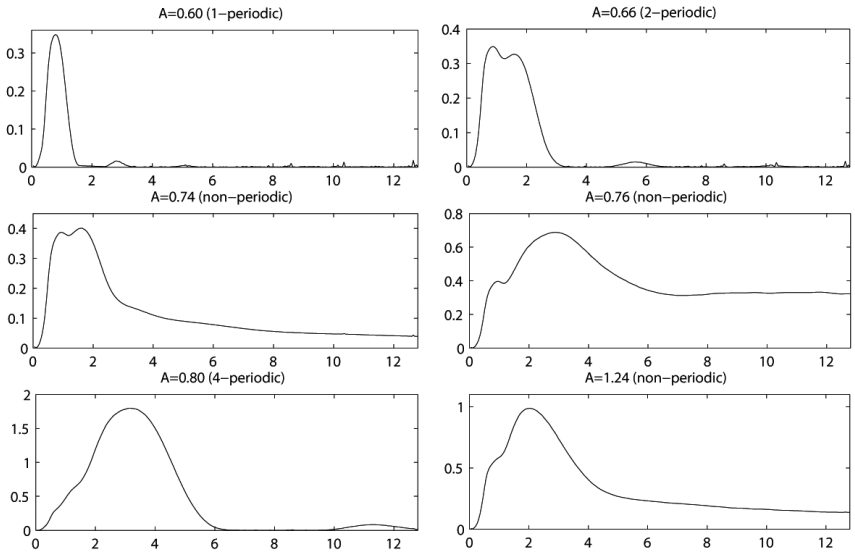

Figure 2: Normalized inner scalograms for certain solutions of the BvP system (Section 4.1), from $t = 20$ to $t = 400$ ($\Delta t = 0.05$), for different values of A, the scale parameter s running from $s_0 = 0.05$ to $s_1 = 12.8$, with $\Delta s = 0.05$, and using Daubechies eight–wavelet function. It is observed how the scalogram of T-periodic signals vanishes at $s = 2T$.

scalogram reaches its maximum value. If the scalogram $\mathcal{S}(s)$ never becomes too small compared to $\mathcal{S}(s_{\max})$ for $s > s_{\max}$, then the signal is "numerically non-periodic" in $[s_0, s_1]$.

Taking into account these considerations, we will define the *scale index* of f in the scale interval $[s_0, s_1]$ as the quotient

$$i_{\text{scale}} := \frac{\mathcal{S}(s_{\min})}{\mathcal{S}(s_{\max})},$$

where $s_{\max}$ is the smallest scale such that $\mathcal{S}(s) \leq \mathcal{S}(s_{\max})$ for all $s \in [s_0, s_1]$, and $s_{\min}$ the smallest scale such that $\mathcal{S}(s_{\min}) \leq \mathcal{S}(s)$ for all $s \in [s_{max}, s_1]$. Note that for compactly supported signals only the normalized inner scalogram will be considered.

From its definition, the scale index i_{scale} is such that $0 \leq i_{\text{scale}} \leq 1$ and it can be interpreted as a measure of the degree of non-periodicity of the signal: the scale index will be zero (or numerically close to zero) for periodic signals and close to one for highly non-periodic signals.

The selection of the scale interval $[s_0, s_1]$ is an important issue in the scalogram analysis. Since the non-periodic character of a signal is given by its behavior at large scales, there is no need for s_0 to be very small. In general, we can choose s_0 such that $s_{\max} = s_0 + \epsilon$ where ϵ is positive and close to zero.

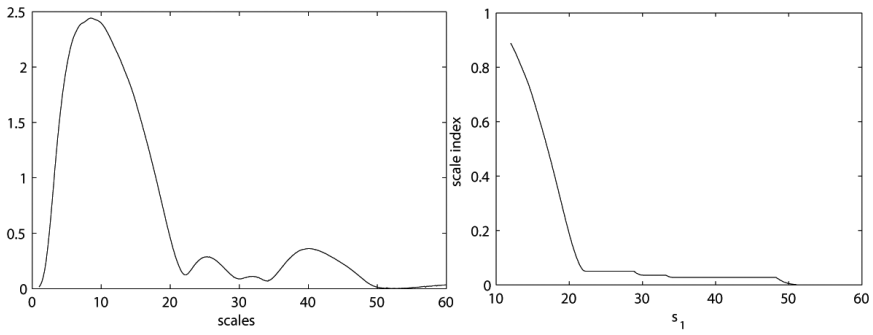

Figure 3: Left: normalized inner scalogram of the almost-periodic function $\sin(t) + \sin\left(t/\sqrt{2}\right) + \sin\left(t/\sqrt{5}\right)$, from $t = 0$ to $t = 800$ ($\Delta t = 0.1$), using the Daubechies four–wavelet function. Right: the scale index tends to zero as we increase the scale s_1.

On the other hand, s_1 should be large enough for detecting periodicities. For example, if we have an almost-periodic function f defined on $\mathbb{R}$, then for any given $\epsilon > 0$ there exists an *almost-period* $T(\epsilon)$ such that

$$|f(t+T) - f(t)| < \epsilon$$

for all $t \in \mathbb{R}$ (see [12]). Hence, if we choose ϵ numerically close to zero, there is a large enough value of T for which the function is "numerically T-periodic",

and the scale index will be close to zero if s_1 is greater than $2T$. So, for an almost-periodic function, the scale index tends to zero as we increase s_1 (see Figure 3). But as s_1 increases, so does the computational cost. In fact, the larger s_1 is, the wider the time span should be where the signal is analyzed, in order to maintain the accuracy of the normalized inner scalogram.

Scales $s_{\min}$ and $s_{\max}$ determine the pattern that the scalogram follows (see Figure 4). For example, in non-periodic signals $s_{\min}$ can be regarded as the "least non-periodic scale". Moreover, if $s_{\min} \simeq s_1$, then the scalogram decreases at large scales and s_1 should be increased in order to distinguish between a non-periodic signal and a periodic signal with a very large period.

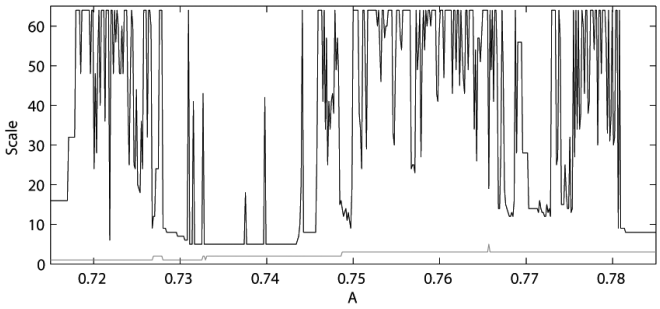

Figure 4: Values of $s_{\max}$ (grey) and $s_{\min}$ (black) for orbits of the BvP oscillator.

4 Examples

In this section we illustrate how the scale index i_{scale} is used in order to detect and study non-periodic orbits of three classical dynamical systems: the logistic map, the Henon map and the forced Bonhoeffer-van der Pol oscillator.

The reason for choosing these dynamical systems as examples for testing the validity of the scale index is mainly that they are three well known chaotic dynamical systems, arising from different research areas, and are mathematically very different. These systems present typical bifurcation diagrams with chaotic and non-chaotic regions. In order to show the effectiveness of the index i_{scale}, we compare the bifurcation diagram, the MLE, and i_{scale}. It will be shown that there is a correspondence between the chaotic regions of the bifurcation diagram, the regions where the MLE is positive, and the regions where i_{scale} is positive.

Figures 5 and 6 depict the comparison between the three methods mentioned above. The signals were studied from $t_0 = 20$ to identify not only periodic signals, but also signals that converge to a periodic one. For the computation of the MLE, 1500 iterations were used. Integer scales between $s_0 = 1$ and $s_1 = 64$ were considered in the computation of i_{scale}. A scale was considered to have no details if the scalogram at that scale takes a value below $\epsilon = 10^{-4}$.

4.1 Continuous Dynamical System: The Bonhoeffer-van der Pol Oscillator

The Bonhoeffer-van der Pol oscillator (BvP) is the non-autonomous planar system

$$\left.\begin{array}{rcl} x' & = & x - \dfrac{x^3}{3} - y + I(t) \\ y' & = & c(x + a - by) \end{array}\right\},$$

being a, b, c real parameters, and $I(t)$ an external force. We shall consider a periodic force $I(t) = A\cos(2\pi t)$ and the specific values for the parameters $a = 0.7$, $b = 0.8$, $c = 0.1$. These values were considered in [13] because of their physical and biological importance (see [14]).

The classical analysis of the BvP system is focused on its Poincaré map, defined by the flow of the system on $t = 1$ (see [1]). Plotting the first coordinate of the periodic fixed points of the Poincaré map versus the parameter A (amplitude of the external force), a bifurcation diagram is obtained [15].

Such diagrams present chaotic and non-chaotic zones. From a geometric point of view, chaos transitions are related to homoclinic orbits (creation or destruction of Smale horseshoes) between the invariant manifolds of a saddle fixed point of the Poincaré map (see [1]). Such a relationship is thoroughly described in a recent work [16].

Figure 5 includes the analysis of the BvP system. The parameter range has been split in two regions, $0.7 \leq A \leq 0.8$ and $1 \leq A \leq 1.3$, which are the regions were chaotic orbits are found. Note the high level of agreement between the MLE and the i_{scale} index: the values of A for which the MLE is negative are also the values for which $i_{\text{scale}} \approx 0$.

Also remarkable is the coincidence between a relative maximum in the i_{scale} and the well known "sudden" expansion of the size of the attractor at $A \approx 0.748$ (see [16], [13]). Moreover, another relative maximum fits with a "sudden" contraction at $A \approx 1.27$.

4.2 Discrete Dynamical Systems: The Logistic and the Henon maps

The logistic map is the discrete dynamical system given by the difference equation

$$x_{t+1} = Ax_t(1 - x_t).$$

This well known dynamical system, arising from population dynamics theory, is a classical example of a simple polynomial map whose orbits exhibit chaotic behavior for some values of the real parameter A.

On the other hand, the Henon map is the two-dimensional dynamical system given by the quadratic map

$$\left\{\begin{array}{rcl} x_{t+1} & = & 1 - Ax_t^2 + y_t \\ y_{t+1} & = & bx_t \end{array}\right. ,$$

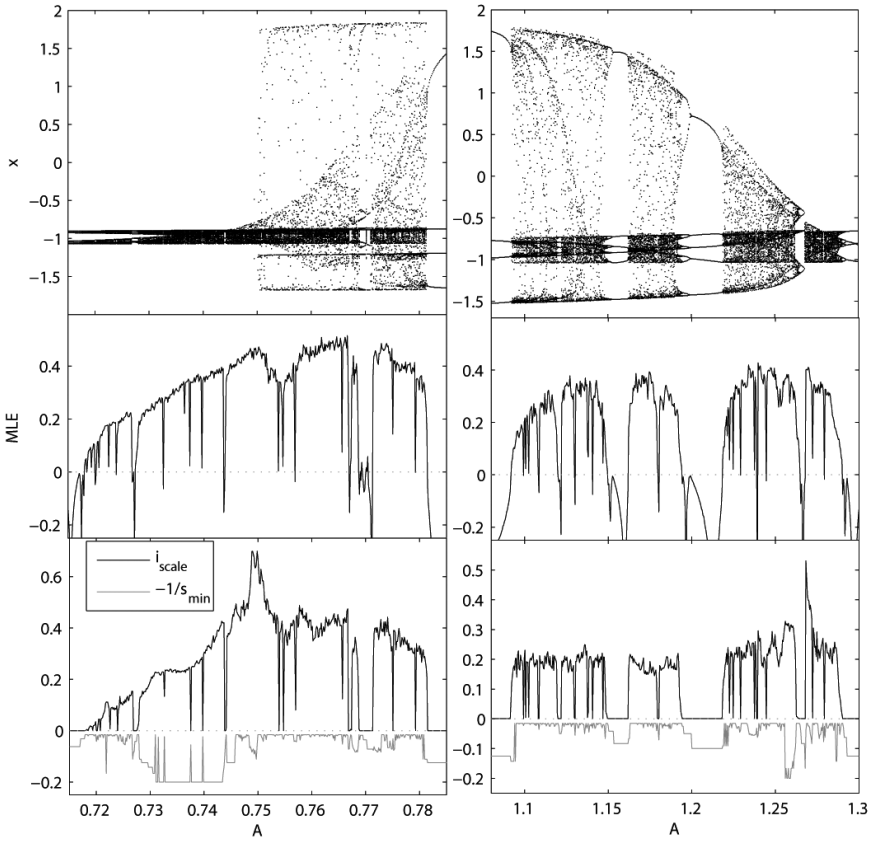

Figure 5: Comparison between the bifurcation diagram, MLE and i_{scale} (from top to bottom) for the BvP oscillator.

with A and b real parameters. For the values $A = 1.4$ and $b = 0.3$, giving what is often called the *canonical Henon map*, a strange attractor is present. Fixing the value $b = 0.3$ and varying the parameter A, the map may be chaotic or not. Through the representation of the x-coordinate of the orbits versus the value of the parameter A, a typical bifurcation diagram is obtained.

Figure 6 shows the comparison between the bifurcation diagram, the MLE and i_{scale} for both the logistic map (left) and the Henon map (right). As in the case of the BvP oscillator, the agreement between the MLE and i_{scale} is clear.

It is also noticeable that the maximum values of the i_{scale} in these two dynamical systems are reached when the main branches of their bifurcation diagrams overlap.

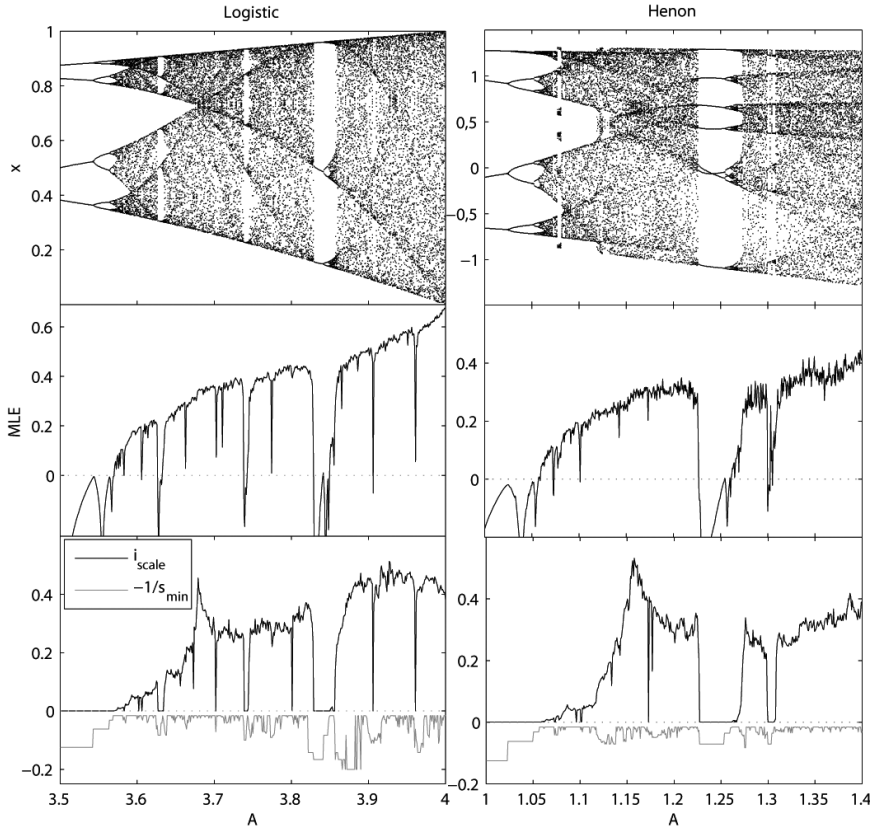

Figure 6: Comparison between the bifurcation diagram, MLE and i_{scale} (from top to bottom) for the logistic map (left) and the Henon map (right).

5 Conclusions

Wavelet analysis has proved to be a valuable tool in the study of chaotic systems. In particular, scalogram analysis and the introduced scale index are a good complement to the MLE, since the scale index gives a measure of the degree of non-periodicity of the signal, while the MLE gives information about the sensitivity to initial conditions. Thus, the combination of the two methods gives us a comprehensive description of a chaotic signal.

Since the MLE and the scale index focus on different characteristics of the signals, the latter contributes to detecting effects that are not detected by the MLE, for example, the sudden expansion of the size of the attractor in the BvP system, and the overlapping of the main branches of the bifurcation diagram in the logistic and Henon maps. Moreover, there are regions in the logistic and Henon graphs where the MLE is increasing but the i_{scale} is decreasing. This means that while the sensitivity to the initial conditions is greater, on the other hand the signal is less non-periodic.

Additionally, the study of the scale index does not require an analytical expression for the signal. In those cases where an analytical description of the dynamical system involved is not available (e.g. experimental signals), although there are methods for estimating the MLE (see [17]), the scale index might be a useful alternative.

These techniques can also be applied to any other discipline where the analysis of time series is required, such as Earth sciences, econometry, biomedicine and any other one where non-linear behavior is expected to occur. For instance, this opens a branch to the study of colour noise presented in this kind of time series; it also could be used to determine properties of seismic and volcanic events ([18]); to detect chaos in non-linear economic time series ([19]) as a complement to other methods already used, like those based on Lyapunov exponents and the power spectral density; and in biomedicine, where wavelets have already been used to analyze non-stationary cardiac signals ([20]).

A Proof of Theorem 1

Given $g : \mathbb{R} \to \mathbb{C}$ with compact support, its periodization over $[0, 1]$ is defined as

$$g^{\text{per}}(t) := \sum_{k \in \mathbb{Z}} g(t + k), \qquad t \in \mathbb{R}.$$

It is clear that, if $g_u(t) := g(t - u)$ is a translated version of g, then

$$(g_u)^{\text{per}}(t) = g^{\text{per}}(t - u). \tag{4}$$

Moreover, if $h \in L^2([0, 1])$, then

$$\langle h^{\text{per}}, g \rangle = \langle h, g^{\text{per}} \rangle_{[0,1]}. \tag{5}$$

Lemma 3 *The periodization $\psi^{per}_{u,s}$ is zero almost everywhere for $u = 0$ and $s = 2$.*

Proof. In this proof we are going to use the dyadic notation for the dilated and translated wavelets given by expression (1). So, we have to prove that $\psi_{j,k}^{\text{per}} = 0$ a.e. for $j = 1$ and $k = 0$.

Let $h \in L^2([0,1])$. Since $\left\{\psi_{j,k}^{\text{per}}\right\}_{-\infty<j\leq 0,\, 0\leq k<2^{-j}} \cup \{1\}$ is an orthogonal basis of $L^2([0,1])$ and the periodization $\psi_{1,0}^{\text{per}}$ is orthogonal to the family of functions $\left\{\psi_{j,k}^{\text{per}}\right\}_{-\infty<j\leq 0,\, 0\leq k<2^{-j}}$ (see [11, Thm. 7.16, Lem. 7.2]), we have

$$\langle h, \psi_{1,0}^{\text{per}}\rangle_{[0,1]} = M\langle 1, \psi_{1,0}^{\text{per}}\rangle_{[0,1]} = M\langle 1, \psi_{1,0}\rangle,$$

where $M = \langle h, 1\rangle_{[0,1]}$. Taking into account that ψ has zero average, we have that $\langle 1, \psi_{1,0}\rangle = 0$, and so

$$\langle h, \psi_{1,0}^{\text{per}}\rangle_{[0,1]} = 0.$$

In general, it can be proved that $\psi_{j,k}^{\text{per}} = 0$ a.e. for all $j \geq 1$ and for all $k \in \mathbb{Z}$.

■

Lemma 4 *The periodization $\psi_{u,2}^{per} = 0$ a.e. for all $u \in \mathbb{R}$.*

Proof. Since $\psi_{u,2}(t) = \psi_{0,2}(t-u)$ we have that $\psi_{u,2}^{\text{per}}(t) = \psi_{0,2}^{\text{per}}(t-u) = 0$ a.e. taking into account (4) and Lemma 3.

■

Theorem 1. *Let $f : \mathbb{R} \to \mathbb{C}$ be a T-periodic function in $L^2([0,T])$, and let ψ be a compactly supported wavelet. Then $Wf(u, 2T) = 0$ for all $u \in \mathbb{R}$.*

Proof. Without loss of generality we may assume that $T = 1$. Then, it will be proved that $Wf(u,2) = 0$ for all $u \in \mathbb{R}$:

Let $h := f|_{[0,1]}$. Then $f = h^{\text{per}}$ and we get

$$Wf(u,2) = \langle f, \psi_{u,2}\rangle = \langle h^{\text{per}}, \psi_{u,2}\rangle = \langle h, \psi_{u,2}^{\text{per}}\rangle_{[0,1]} = 0,$$

taking into account (5) and Lemma 4.

■

Acknowledgments

We thank Carlos Fernández García, the referees, and the editor of the journal *Computer and Mathematics with Applications* for their useful comments and suggestions that improved the paper.

References

[1] J. Guckenheimer, P. Holmes. *Nonlinear Oscillations, Dynamical Systems and Bifurcations of Vector Fields*. Applied Mathematical Sciences, 42. Springer-Verlag (1983).

[2] S. H. Strogatz. *Nonlinear Dynamics and Chaos: with applications to physics, biology, chemistry and engineering.* Addinson-Wesley (1994).

[3] C. Chandre, S. Wiggins, T. Uzer, Physica D **181**, 171 (2003).

[4] B. Donald, P. Walden, A. T. Walden, *Wavelet Methods for Time Series Analysis*, Cambridge University Press, (2000).

[5] F. Tony, C. Shen, J. Shen, *Image Processing and Analysis - Variational, PDE, Wavelet, and Stochastic Methods*, Society of Applied Mathematics, (2005).

[6] A. Arneodo, B. Audit, J. F. Muzy, S. G. Roux, Physica A **254**, 24-45 (1998).

[7] J. Poligiannakis, P. Preka-Papadema, X. Moussas, Mon. Not. R. Astron. Soc. **343**, 725-734 (2003).

[8] P. K. Panigrahi,P. Manimaran, A. Lakshmi, R. R. Yadav, ArXiv:abs/nlin/0604002 (2006).

[9] D. Permann, I. Hamilton, Phys. Rev. Lett. **69**, 2607 (1992).

[10] M. Lakestani, M. Razzaghi, M. Dehgham, Phys. Scripta. **74**, 362 (2006).

[11] S. Mallat, *A wavelet tour of signal processing.* Academic Press London (1999).

[12] H. Bohr, *Almost-periodic functions.* Chelsea, reprint (1947).

[13] S. Rajasekar. Chaos, Solitons & Fractals, **7**, 1799 (1996).

[14] A. C. Scott. *Neurophysics.* Wiley, New York (1977).

[15] W. Wang. J. Phys. A, **22**, L627 (1989).

[16] R. Benítez, V. J. Bolós, Chaos, Solitons & Fractals, **40**, 2170 (2009).

[17] X. Zeng, R. Eykholt, R. A. Pielke, Phys. Rev. Lett. **66**, 3229 (1991).

[18] J. M. Ibáñez et al. J. Volcanol. Geotherm. Res. **128**, 65-88 (2003).

[19] W. A. Barnett, M. J. Hinich, Annals of Operations Research **37**, 1 (1992).

[20] O. Faust, R. Acharya, S.M. Krishnan, L. Choo Min, BioMedical Engineering OnLine, 3:30 (2004).